COBEM 2023 27TH INTERNATIONAL CONGRESS OF MECHANICAL ENGINEERING

ABCM Brazilian Society of Mechanical Sciences and Engineering
27th ABCM International Congress of Mechanical Engineering
December 04-08, 2023, Florianópolis-SC, Brazil

COB-2023-0521
EXPERIMETAL DETERMINATION OF METHANE DIFFUSIVITY IN WATER AND BRINE UNDER HYDRATE FORMATION CONDITIONS

Thales H. Sirino
Celina Kakitani
Luiz F. S. Vasconcelos
João V. M. Rocha
Dalton Bertoldi
Rigoberto E. M. Morales
Moisés A. Marcelino Neto
Multiphase Flow Research Center – NUEM, Graduate Program in Mechanical and Materials Engineering – PPGEM, Federal University of Technology of Parana, Brazil
thaleshsirino@hotmail.com
celinak@utfpr.edu.br
luizvasconcelos@alunos.utfpr.edu.br
joaorocha.2019@alunos.utfpr.edu.br
daltonbertoldi@utfpr.edu.br
mneto@utfpr.edu.br
rmolares@utfpr.edu.br

Abstract. *The objective of this study is to experimentally determine the diffusivity of methane in water and brine under hydrate formation conditions using the pressure decay method. To reduce the simplifications necessary for determining mass transfer parameters, which may lead to potential errors or limit its applicability, a numerical model that considers diffusivity dependent on solute concentration and liquid phase swelling was developed. Quasi-equilibrium and mass balance based boundary conditions were used at the gas-liquid interface, with the saturation concentration of the solute obtained through a flash calculation using the Cubic-Plus-Association equation of state (CPA). The equation of state also provided the mixture density and gas fugacity coefficient, enabling the use of a thermodynamic correction factor for refining diffusivity. Experiments were conducted at 277.15 K and pressures ranging from 45 bar to 50 bar, with salt concentrations up to 3.5% in mass fraction.*

Keywords: *Diffusivity, Pressure decay, Hydrate, Concentration-dependent diffusivity, Swelling, Cubic-Plus-Association.*

1. INTRODUCTION

Hydrates are solids composed by water molecules interconnected through hydrogen bonds that forms a crystalline structure capable of occluding small molecules, usually light hydrocarbons. The hydrate formation process occurs under conditions of low temperatures and high pressures, scenarios that are commonly observed in oil and gas production processes in deep water. Unfortunately, the formation of these solids poses significant challenges, as they can agglomerate and obstruct pipelines, resulting in productivity and financial losses, equipment damage, and environmental, safety, and health risks. Consequently, the oil and gas industry implements numerous measures to mitigate potential damage. One effective strategy involves injecting kinetic inhibitors to delay crystal formation and growth. However, the successful application of this technique requires a comprehensive understanding of the hydrate formation process (Sloan and Koh,2008).

From a molecular perspective, hydrate growth is a result of three interplaying factors: the kinetic growth of crystals on the hydrate surface, mass transfer of components to the crystal growth surface, and dissipation of the heat of formation away from the growing crystal surface. The hydrate phase can accommodate up to 15 mol% of gas, significantly exceeding the solubility of methane in water by at least two orders of magnitude. Hence, it becomes evident that the gas transport to the hydrate surface becomes of utmost importance and can govern the entire process (Sloan and Koh,2008). And one of the most important parameters that governs the mass transfer processes is the diffusivity.

Diffusivity is the parameter typically used in defining dimensionless numbers employed to describe various mass transfer phenomena. Moreover, both gas absorption in liquids and mass transfer from liquids to solids depend on diffusivity (Cussler, 2009). As a result, many kinetic models of hydrate formation have a direct dependence on diffusivity. In the literature, there are limited studies focusing on the diffusion of hydrate-forming gases in liquids within high-pressure and low-temperature. The vast majority of works examine the diffusion process under reservoir conditions,

meaning higher temperatures, as a significant portion of these studies focus on heavy oil recovery. Thus, considering this scenario, it becomes necessary to study and obtain mass transfer parameters, such as diffusivity, under hydrate formation conditions to feed hydrate´s kinetic models accurately. Through reliable parameters and a deeper understanding of mass transfer processes under these conditions, it becomes easier to identify the limiting steps in the entire process of hydrate formation.

There is no equipment capable of directly measure the diffusivity or even a consolidated theoretical approach for its determination. Nevertheless, there are properties that can be experimentally measured and correlated to diffusivity through models. Several authors have proposed different experimental methodologies and calculation methods based on conservation equations and semi-empirical relations to estimate diffusivity. However, these solutions incorporate assumptions and simplifications that may limit its applicability or impose a potential error. One of the most used approaches is the application of the continuity equation in a system where the diffusion process is taking place. And to apply the continuity equation is necessary to know the species composition over space and time. The compositions and concentration gradients in the system can be measured directly, however direct measurement methods are relatively expensive and often intrusive (Sheikha et al., 2005). Then came the need to develop simpler experimental methodologies. Among all the different experimental methods used to determine the diffusivity of gases in liquids, the pressure decay method developed by Riazi (1996) is the most widely applied due to its precision, simplicity, and convenience (Rasmussen and Civan, 2009).

The method essentially involves placing a gas phase and a liquid phase in contact within a constant-volume PVT cell at a specific initial pressure and temperature. The temperature remains constant throughout the experiment, and as the gas diffuses into the liquid phase, there is a decrease in the pressure of the gas phase, which is monitored and recorded. If the experiment is conducted long enough, at a certain point, the pressure will no longer decrease, and the system will have reached a state of thermodynamic equilibrium, known as saturation. Therefore, as a result of the pressure decay method, it is also possible to obtain the gas solubility in the liquid at the temperature of the conducted experiment. As can be observed, from an experimental standpoint, the methodology is truly simple and cost-effective, making it attractive. After conducting the experiments, the pressure profile over time is obtained, where the pressure decay correlates to the mass of gas diffusing across the cross-sectional area of the gas-liquid interface during the considered interval. And applying the continuity equation it is possible to determine de diffusivity of the gas in the liquid phase.

One of the main challenges of this method lies in appropriately modeling the gas-liquid interface, especially the solute concentration at the liquid interface surface and its dependence on pressure over the course of the experiment, as well as describing the variation of other pressure-dependent properties like density, compressibility factor, etc. According to Khalifi (2021), one of the main disadvantages of the pressure decay method is its high dependence on the validity of the employed equation of state and the description of interface properties. Unlike Riazi's work (1996), which used the Peng-Robinson equation of state, most studies using the pressure decay technique rely on empirical or semi-empirical correlations to determine parameters such as solute concentration, density, compressibility factor, etc. This simplifies the implementation of the mathematical model. In this study were implemented a quasi-equilibrium and a mass balance-based boundary conditions at the gas-liquid interface. The methane saturation concentrations during the entire experiment were obtained through a flash calculation using the Cubic-Plus-Association equation of state. The equation of state was also utilized to determine the fugacity coefficient necessary for the application of the thermodynamic correction factor, as well to estimate the density variation of the aqueous solution during the diffusion process (swelling).

2. EXPERIMENTAL METHODOLOGY

2.1 Experimental Apparatus

The experimental setup was designed and assembled in the Flow Assurance Laboratory of the Multiphase Flow Center (NUEM), located within the Federal University of Technology - Paraná (UTFPR). As depicted in Figure 1, it consists of a gas cylinder (1) connected to a syringe pump (2), responsible for injecting gas into the PVT cell (3). The temperature is maintained constant throughout the experiment using a thermostatic bath (4). Once the desired pressure inside the cell is reached, and gas injection is stopped, the valve (5) is closed. The pressure inside the cell is continuously monitored throughout the experiment by a pressure transducer (6), and the pressure data over time is stored on a computer (7). Before gas injection, the entire system is subjected to vacuum to ensure there is no dissolved contaminant gas in the liquid or trapped inside the lines and cell. A vacuum pump (8) is activated to achieve this vacuum.

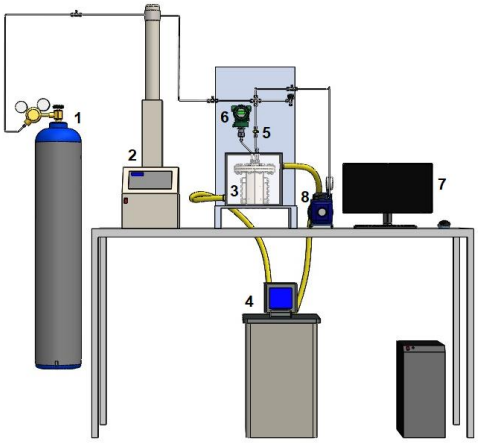

Figure 1. Schematic representation of the experimental apparatus.

The PVT cell, shown in Figure 2, functions as the reservoir where the diffusion process occurs. It has an internal diameter of 70 mm and an internal height of 160 mm. Two polycarbonate viewing windows, each with a height of 100 mm and an internal curvature matching a diameter of 70 mm, were attached to it. These windows serve the purpose of enabling continuous monitoring of the liquid phase's swelling as the diffusion process unfolds.

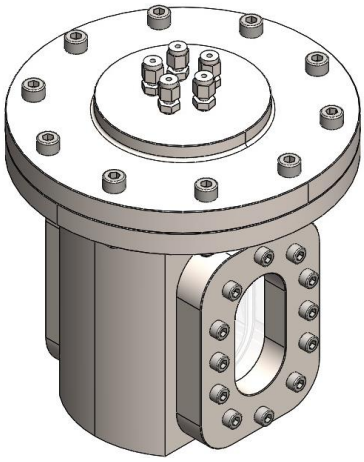

Figure 2. PVT Cell.

Figure 3 provides an illustrative depiction of the interior of the PVT cell, with a focus on the gas-liquid interface and the thermoresistances. As can be observed, three PT-100 thermoresistances are strategically positioned in different parts of the system. One is located in the gas phase, another at the gas-liquid interface, and the last one in the middle of the solvent. The use of these three thermoresistances in different locations is to monitor the effect of gas dissolution enthalpy in the liquid within these regions. Particularly, the PT-100 located in the liquid phase supplies valuable information on when the gas diffusion front reaches the height of the liquid where it is positioned. This is indicated by a temperature increase, caused by the heat release upon the arrival of the diffusion front.

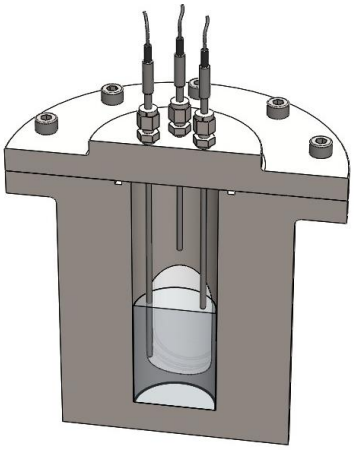

Figure 3. PVT cell interior.

The instrumentation comprises a Yokogawa pressure transducer, model EJX510A-JCS4N012EL, operating in the pressure range of 0 to 100 bar with an accuracy of 0.04 bar. In addition to the pressure transducer, there are three Omega thermoresistances, model P-M-1/10-1/8-6-0-P-3, designed to work in the temperature range of -50 to 250 °C with a precision of 1/10 DIN.

2.2 Experimental Procedure

The first step is to perform a leakage test before commencing the experiments. This test involves pressurizing the entire system, including the PVT cell and all connections, with the gas under study, and monitoring the pressure for 7 days. Additionally, a leak detection liquid is used on all frequently disconnected parts to specifically check critical connections.

After confirming the absence of leaks, all test gas is purged from the system, and a known mass of solvent is added to the PVT cell, sufficient to achieve a height of approximately 50 mm inside the cell. Then, a vacuum is applied to ensure no contaminants remain trapped in the lines or dissolved in the solvent. Next, the bath temperature is set to the desired value, and the system is left undisturbed until the next day to achieve thermal equilibrium. Finally, the gas is injected into the PVT cell at the determined pressure, with controlled flow to avoid advection upon contact with the liquid and minimize significant diffusion during filling.

Over time, the gas diffuses into the liquid, causing a gradual decrease in system pressure. The pressure is continuously monitored throughout the experiment using the pressure transducer installed in the PVT cell, along with gas phase, interface, and liquid midpoint temperatures. A computer connected to a data acquisition system saves the measured pressure every minute. The experiment concludes when the pressure variation is less than the uncertainty of the pressure transducer measurement or if it reach 20 days.

Table 1 lists all materials used in the tests, followed by their CAS number, suppliers, and supplier purity. No additional refining method has been used.

Table 1. Used Components, CAS Registry Number, Supplier, and Purity.

Components	CAS reg. no.	Supplier	Purity
Methane	74-82-8	White Martins	≥0.995
Sodium Chloride	7647-14-5	Dinâmica	≥0.995
Distilled Water	7732-18-5		

3. DIFFUSIVITY MODELING

The pressure decay method, as explained earlier, involves the diffusion of a gas in a liquid column, as shown in Figure 4. The gas is absorbed at the gas-liquid interface, z=0, and diffuses until it reaches the bottom of the column, z=h(t). Under dilute conditions, the total liquid height remains relatively constant. However, at high concentrations of the diluted gas, swelling of the liquid phase occurs, resulting in an increase in the column height. In the developed model, the gas-liquid interface remains defined at the domain origin, and the change in height is accounted for in its length, h(t).

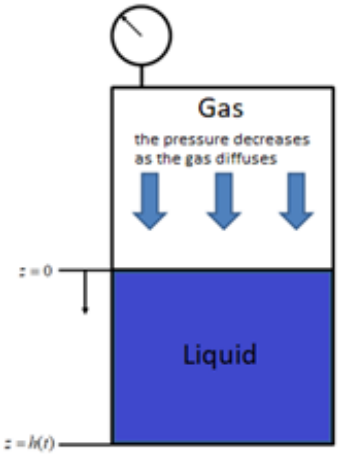

Figure 4. Representation of the diffusive process.

The mass transfer in a control volume can be described by the general continuity equation:

$$\frac{\partial c_A}{\partial t} = -\nabla\left(c_A\vec{v}\right) - \nabla\left(\vec{j_A}\right) + r_A, \tag{1}$$

$$\vec{j_A} = -D_{AB}\nabla(c_A), \tag{2}$$

Where c_A is the mass concentration in Kg/m^3, $\vec{v}$ the advection velocity in m/s, $\vec{j_A}$ the diffusive mass flux in Kg/m^{2}s, t is the time in seconds, and D_{AB} is the diffusivity in m^2/s. The first step in solving the continuity equation is the appropriate simplification of the problem according to the analyzed system, its geometry, and experimental conditions. Then, the initial and boundary conditions are chosen and applied to the simplified continuity equation to determine the concentration profile of the gas in the liquid and the total mass of solute diffused over time. With this data, it is possible to estimate the pressure drop during the experiment and compare it with the pressure profile obtained experimentally. However, to perform these calculations, it is necessary to know the value of the diffusivity. Thus, during the calculation procedure, the assigned value of diffusivity varies until the respective pair is found that best describes the variation of the pressure obtained experimentally.

In this work, the following assumptions have been considered in the mathematical modeling:

- The water is a non-volatile liquid. Therefore, mass transfer cannot happen from the oil to the gas phase.
- No chemical reaction occurs and the absorption is purely a physical process.
- The process is assumed to be isothermal.
- The mass transfer from gas to water is only due to molecular diffusion. No convection is considered.
- The effect of capillary pressure is neglected, and hence the interface between methane and water is considered to be flat.
- Liquid swelling takes place as methane gas dissolves in the water.
- The methane diffusion coefficient in water is considered not constant over the concentration range in the experiment (application of a thermodynamic correction factor).

After applying all these considerations, the continuity equation can be rewritten as follows:

$$\frac{\partial c_A}{\partial t} = \frac{\partial}{\partial z}\left(D_{AB}\frac{\partial c_A}{\partial z}\right), \tag{3}$$

It is worth noting that in this work, the continuity equation, Eq. (3), does not take the form of Fick's second law due to the dependence of diffusivity on the solute concentration. Therefore, the diffusivity varies along the z-axis. This dependence on the solute concentration is computed through the implementation of the thermodynamic correction factor (α):

$$D_{AB} = \bar{D}_{AB}\left(\frac{\partial \ln \Phi_A}{\partial \ln x_A}\right)_{T,P} = \alpha\bar{D}_{AB}, \tag{4}$$

Where $\bar{D}_{AB}$ is the Maxwell-Stefan diffusivity, Φ_A the fugacity coefficient and x_A the mole fraction.

To solve the continuity equation, Eq. (3), the application of an initial condition and two spatial boundary conditions is required. The initial condition employed in the model assumes an absence of gas concentration within the solvent at

the outset. To validate this initial state and ensure that no diluted methane remains in the liquid phase prior to commencing the experiment, a vacuum is applied to the system before introducing the gas and initiating the test. This initial condition is mathematically represented by Eq. (5).

$$c_A(z, t = 0) = 0, \tag{5}$$

In this study, two different boundary conditions were tested for the gas-liquid interface. The first one is called the quasi-equilibrium boundary condition, which is represented by Eq. (6). Initially, this boundary condition was chosen for the system because it is a specific case of a more general condition proposed by Etminam et al. (2013). The general time-dependent non-equilibrium boundary condition simplifies to the quasi-equilibrium condition in systems with high resistance to mass transfer at the interface. This is the case for methane and water, where the molecules are quite different and lack chemical affinity.

$$c_A(z, t)|_{z=0} = c_{sat}(P(t)) \therefore t > 0, \tag{6}$$

Where c_{sat} is the saturation concentration. In this work, a flash calculation was implemented in order to determine the solute's saturation concentration throughout the experiment based on the pressure reported in the system. And the same flash calculation can be used to determine the mass flow rate (dm_A/dt) that passes through the interfacial film. Therefore, Eq. (7), was also used as a boundary condition at the interface.

$$\frac{dm_A}{dt} = -D_{AB} A \frac{dc_A}{dz}\Big|_{z=0}, \tag{7}$$

Lastly, the final boundary condition is related to the bottom of the column. As the bottom of the solvent column is in contact with a metallic surface of the PVT cell, there will be no gas diffusion from this position. Consequently, the concentration gradient is zero at this point, and the boundary condition is defined by Eq. 8.

$$\frac{dc_A}{dz}\Big|_{z=h} = 0, \tag{8}$$

In the numerical model, the liquid phase is divided into equal-thickness layers, and the gas phase is considered to be homogeneous, as shown in Figure 5. The initial solute concentration in each layer is defined as zero. A quasi-equilibrium or a mass balance-based boundary is condition applied at the gas-liquid interface, while the no-flux condition is implemented at the bottom of the liquid column.

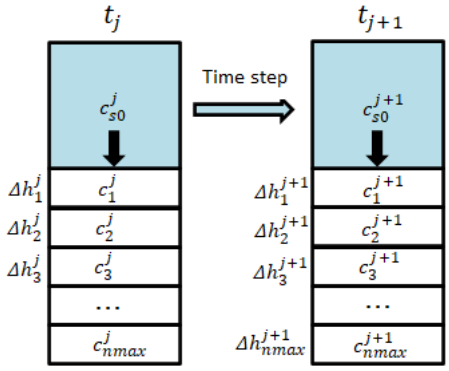

Figure 5. Numerical model for pressure decay experiments.

At each time step, the solute diffusion from one layer to another in the liquid phase is determined by the continuity equation with the presence of the non-constant and concentration-dependent diffusivity, as expressed in Eq. (3). The diffusivity is corrected using a thermodynamic correction factor, Eq. (4), which is a function of the solute fugacity coefficient. The liquid mass is kept constant in each cell, with variations occurring only in the solute mass. The density of each layer is determined, and the cell height is recalculated accordingly. The total diffused mass is the sum of the masses in each cell, and the gas-liquid interface height is the sum of the heights of all the layers. The equations were discretized using the FTCS method, which is progressive in time and centered in space.

The Cubic-Plus-Association (CPA) equation of state was employed to perform the flash calculation, estimate the density of the aqueous solution, and determine the methane fugacity coefficient in the aqueous for the thermodynamic correction factor. The CPA equation of state was chosen because it was developed by Kontogeorgis et al. (1996) with the aim of improving the predictive accuracy of cubic equations of state in systems containing associating compounds. One

of the main challenges related to the use of a thermodynamic correction factor lies precisely in its application to systems with associations, as many models developed for estimating concentration-dependent diffusivity yield unsatisfactory results for such systems (Poiling et al., 1987). Since one of the systems analyzed in this study contains an associating compound, water, it becomes important to use an equation of state that takes into account these associating forces (hydrogen bonds) when determining the fugacity coefficient. For details of the Flash calculation routine implemented in this work, consult the work by Sirino et al. (2018).

The model estimates diffusivity values and reconstructs the pressure profile based on the selected diffusivity value. After completing the calculations, a comparison is conducted between the calculated and experimental pressure profiles using Eq. 9.

$$F_{obj} = \frac{1}{n}\sum_1^j \left| \frac{P_{cal}^j - P_{exp}^j}{P_{exp}^j} \right|, \tag{9}$$

Where F_{obj} is the average relative deviation of the calculated pressure (P_{cal}^j) at time instant *j* from the experimental pressure (P_{exp}^j). The diffusivity is optimized by an iterative process until the F_{obj} value is minimized. The optimization method used was Nelder-Mead.

4. RESULTS AND DISCUSSION

This section will showcase the experimental results and the calculated diffusivities for two distinct systems at a temperature of 277.15 K. This temperature was chosen to simulate conditions found in the depths of the ocean floor. The first system comprises methane and pure water, while the second system includes methane and a saline aqueous solution containing 3.5 wt% of NaCl. This salt concentration was also selected to replicate the salinity commonly found in oceans.

Prior to calculating the diffusivity, it was necessary to ensure that flash calculation was determining accurately the saturation concentration and density of the mixtures. For the methane and water system, the binary interaction parameter (k_{ij}) between these two components was optimized, taking into account experimental studies on methane solubility in water (Wang et al., 1995; Lekvam et al. 1997; Yang et al., 2001; Servio and Englezos, 2002; Wang et al., 2003; Chapoy et al., 2003; Kim et al., 2003; Chapoy et., 2004; Frost et al., 2014). It was assumed that the binary interaction parameter has a linear dependence on temperature, and the optimized value is given by Eq. (10).

$$k_{ij} = 0.00291245T - 0.86904398, \tag{10}$$

In the optimization, 120 experimental data points of methane solubility in water were used, with temperatures ranging from 274.19 K to 326.56 K. The relative average deviation between the experimental data and the calculated solubilities was 4.07 %. For further details on the binary interaction parameters optimization routine, refer to the works of Jacomel et al., (2019) and Sirino et al., (2018).

For the water and brine system, the influence of salts on the bulk equilibrium properties was taken into account using the methodology introduced by Aasberg-Petersen et al. (1991) and extended to the CPA equation of state by Haghighi et al. (2008). The interaction parameters between the electrolyte and the non-electrolyte component (h_{is}) were also optimized, assuming a linear dependency on temperature. The interaction parameter between NaCl and water was adjusted based on experimental data of density for saline solutions, while data on methane solubility in NaCl aqueous solutions were used to tune the interaction parameter between NaCl and methane. The obtained results can be observed in Eq. (11) and Eq. (12).

$$h_{H2O-NaCl} = 1.37386823 * 10^{-5}T - 1.37734475 * 10^{-2}, \tag{11}$$

$$h_{CH4-NaCl} = -0.00164019T + 0.53015396, \tag{12}$$

The experimental data for the density of aqueous NaCl solutions, utilized in optimizing the binary interaction parameter between water and NaCl, were extracted from the study by Al Ghafri et al. (2012). The data encompassed temperatures ranging from 283 to 432 K, pressures up to 68.5 MPa and salt concentration molality ranging from 1.06 to 6m. The average relative deviation between the experimental data points and the calculated densities was 2.3%.

The experimental data for methane solubility in aqueous NaCl solutions, used to optimize the interaction parameter between methane and NaCl, were extracted from the works of Stoessell and Byrne (1982) and Sullivan and Smith (1970). The salt concentration in these studies ranged from 0.5 to 4m, while the temperature varied from 298K to 324.65 K and pressures reached up to 600 bar. The average relative deviation between the experimental data points and the calculated solubilities was 1.29%.

After validating the Flash calculation, specifically the required parameters such as solubility and density, the diffusivity was determined. Figure 9 presents the experimentally obtained pressure profile for the methane-water system at 277.15 K and an initial pressure of approximately 45 bar, falling within the hydrate formation envelope. Figure 9 also includes four pressure profiles reproduced through mathematical modeling. Among these, two curves assume a constant diffusivity, distinguished by the boundary condition adopted at the gas-liquid interface. One curve applies the quasi-equilibrium boundary condition (A), while the other uses the mass balance-based boundary condition (B). The remaining two curves also employ the quasi-equilibrium and mass balance-based boundary conditions, respectively, but with the added implementation of the thermodynamic correction factor (+).

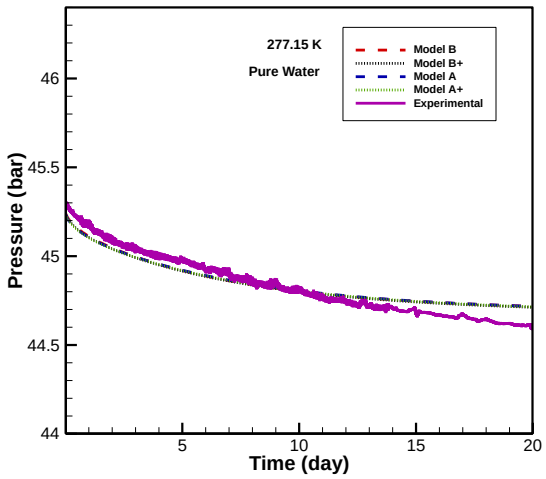

Figure 9. Experimental and calculated pressure profiles for the methane and water system at 277.15 K.

As observed in Table 2, the diffusivities obtained from models (A+ and B+), which considered the influence of concentration on diffusivity, demonstrated higher values compared to models (A and B) that applied the same boundary conditions but without the thermodynamic correction factor. This outcome was anticipated since methane diffuses into water, and as its concentration increases in the aqueous medium, its diffusivity decreases. Consequently, the Fickian diffusivity should assume a higher value under these circumstances. Since the solubility of methane in water is very low, the values obtained for diffusivity did not vary significantly with the implementation of the thermodynamic correction factor. In such cases, where conditions approach infinite dilution, it is common to assume that diffusivity remains independent of concentration. Nevertheless, for both boundary conditions, the implementation of the thermodynamic correction factor slightly improved the model's performance. The mass balance-based boundary conditions also exhibited slightly better accuracy compared to the quasi-equilibrium boundary condition curves.

Table 2. Comparison between the diffusivity values obtained for the methane and water system at 277.15 K.

Mathematical modeling	**D (m^2/s)**	**Relative average deviation**
Model A	$6.95x10^{-10}$	0.1085%
Model B	$7.10x10^{-10}$	0.1081%
Model A+	$7.25x10^{-10}$	0.1071 %
Model B+	$7.50x10^{-10}$	0.1066%

Figure 10 displays pressure profiles obtained through the methane diffusion process in brine (3.5 wt% NaCl) at a temperature of 277.15 K and an initial pressure of approximately 50 bar. Similar to Figure 9, the letter A in the models refers to the quasi-equilibrium boundary condition at the gas-liquid interface, while the letter B represents the mass balance-based boundary condition. Additionally, the symbol "+" indicates the implementation of the thermodynamic correction factor in the models.

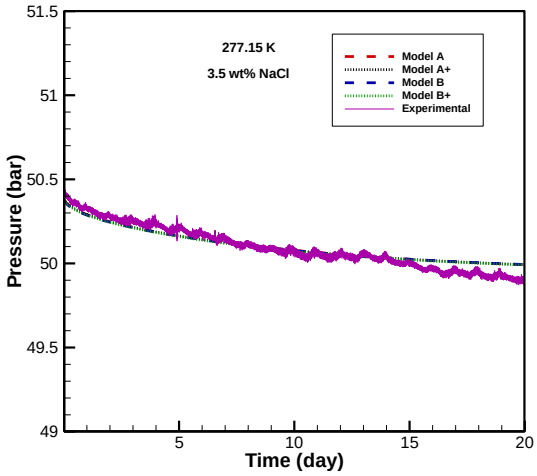

Figure 10. Experimental and calculated pressure profiles for the methane and brine system (3.5 wt% NaCl) at 277.15 K.

Table 3 presents the diffusivities obtained for the methane and brine system. Just like in the methane and water system, the models that utilized the thermodynamic correction factor exhibited slightly enhanced performance compared to the models without its implementation. Moreover, the diffusivity values obtained also showed an increase compared to systems where diffusivity remains unaffected by solute concentration. Additionally, it can be observed that the diffusivity values obtained for the system containing a saline aqueous solution were lower compared to those obtained for the system containing only pure water. This can be attributed to the phenomenon commonly known as salting out. In general terms, salting out refers to the decrease in solubility of a nonelectrolyte compound, such as methane in this case, as the concentration of a salt increases in water.

Table 3. Comparison between the diffusivity values obtained for the methane and brine (3.5 wt% NaCl) system at 277.15 K.

Mathematical modeling	**D (m^2/s)**	**Relative average deviation**
Model A	$5.32x10^{-10}$	0.0650%
Model B	$5.26x10^{-10}$	0.0633%
Model A+	$5.55x10^{-10}$	0.0646 %
Model B+	$5.35x10^{-10}$	0.0630%

5. CONCLUSION

Diffusivity plays a critical role in mass transfer calculations and velocity-controlled processes. Despite its significance, the literature offers limited experimental diffusivity measurements, primarily due to the time-consuming and costly nature of such experiments. Moreover, the few studies exploring the diffusivity of light hydrocarbons in liquids have primarily focused on high-pressure and high-temperature conditions, rather than addressing temperatures where hydrate formation risks are present. Given that diffusivity is a crucial parameter in kinetic models of hydrate formation, this study successfully generated important experimental data on methane diffusivity in water and brine under conditions conducive to hydrate formation. The values obtained for the diffusivity of methane in water at 274.15 K were similar to the value of $7.02x10^{-10}$ obtained by Guo et al. (2013) at a temperature of 273 K using In situ Raman spectroscopy. This demonstrates that the experimental methodology applied in this study, despite being simpler and more cost-effective, yielded satisfactory results compared to other more complex and expensive methodologies.

The development of the model also brings some contributions to the literature. Firstly, it involves conducting a flash calculation at each time step to determine the concentration at the gas-liquid interface using a mass balance-based boundary condition. Furthermore, the model utilizes this flash calculation routine and the equation of state implemented to estimate the density variation of the liquid solution, along with determining a thermodynamic correction factor. The equation of state itself applied in the model can be considered a distinctive feature, as it is an associative equation of state known as Cubic-Plus-Association (CPA), developed with the purpose of enhancing the predictive accuracy of cubic equations of state in systems that contain associative compounds. Considering that the systems analyzed in this study contains water, it becomes advantageous to use an equation of state that takes these associative forces (hydrogen bonding) into account in determining the fugacity.

6. REFERENCES

Aasberg-Petersen, K., Stenby, E., & Fredenslund, A. (1991). Prediction of high-pressure gas solubilities in aqueous mixtures of electrolytes. Industrial & engineering chemistry research, 30(9), 2180-2185.

Al Ghafri, S., Maitland, G. C., & Trusler, J. M. (2012). Densities of aqueous MgCl2 (aq), CaCl2 (aq), KI (aq), NaCl (aq), KCl (aq), AlCl3 (aq), and (0.964 NaCl+ 0.136 KCl)(aq) at temperatures between (283 and 472) K, pressures up to 68.5 MPa, and molalities up to 6 mol· kg–1. Journal of Chemical & Engineering Data, 57(4), 1288-1304.

Chapoy, A., Coquelet, C., & Richon, D. (2003). Solubility measurement and modeling of water in the gas phase of the methane/water binary system at temperatures from 283.08 to 318.12 K and pressures up to 34.5 MPa. Fluid phase equilibria, 214(1), 101-117.

Chapoy, A., Mohammadi, A. H., Richon, D., & Tohidi, B. (2004). Gas solubility measurement and modeling for methane–water and methane–ethane–n-butane–water systems at low temperature conditions. Fluid phase equilibria, 220(1), 113-121.

Cussler, E. L. (2009). Diffusion: mass transfer in fluid systems. Cambridge university press.

Etminan, S. R., Pooladi-Darvish, M., Maini, B. B., & Chen, Z. (2013). Modeling the interface resistance in low soluble gaseous solvents-heavy oil systems. Fuel, 105, 672-687.

Frost, M., Karakatsani, E., von Solms, N., Richon, D., & Kontogeorgis, G. M. (2014). Vapor–liquid equilibrium of methane with water and methanol. Measurements and modeling. Journal of Chemical & Engineering Data, 59(4), 961-967.

Guo, H., Chen, Y., Lu, W., Li, L., & Wang, M. (2013). In situ Raman spectroscopic study of diffusion coefficients of methane in liquid water under high pressure and wide temperatures. Fluid Phase Equilibria, 360, 274-278.

Haghighi, H., Chapoy, A., & Tohidi, B. (2008). Freezing point depression of electrolyte solutions: experimental measurements and modeling using the cubic-plus-association equation of state. Industrial & engineering chemistry research, 47(11), 3983-3989.

Jacomel, F. C., Sirino, T. H., Marcelino Neto, M. A., Bertoldi, D., & Morales, R. E. (2019). Loss of methanol and monoethylene glycol in VLE and LLE: prediction of hydrate inhibitor partition. Journal of Chemical & Engineering Data, 64(9), 3889-3903.

Khalifi, M. (2021). Experimental Measurement of Diffusion Coefficient of Gaseous Solvents in Liquids.

Kim, Y. S., Ryu, S. K., Yang, S. O., & Lee, C. S. (2003). Liquid water− hydrate equilibrium measurements and unified predictions of hydrate-containing phase equilibria for methane, ethane, propane, and their mixtures. Industrial & Engineering Chemistry Research, 42(11), 2409-2414.

Kontogeorgis, G. M., Voutsas, E. C., Yakoumis, I. V., & Tassios, D. P. (1996). An equation of state for associating fluids. Industrial & engineering chemistry research, 35(11), 4310-4318.

Lekvam, K., & Bishnoi, P. R. (1997). Dissolution of methane in water at low temperatures and intermediate pressures. Fluid Phase Equilibria, 131(1-2), 297-309.

O'Sullivan, T. D., & Smith, N. O. (1970). Solubility and partial molar volume of nitrogen and methane in water and in aqueous sodium chloride from 50 to 125. deg. and 100 to 600 atm. The Journal of Physical Chemistry, 74(7), 1460-1466.

Rasmussen, M. L., & Civan, F. (2009). Parameters of gas dissolution in liquids obtained by isothermal pressure decay. AIChE journal, 55(1), 9-23.

Riazi, M. R. (1996). A new method for experimental measurement of diffusion coefficients in reservoir fluids. Journal of Petroleum Science and Engineering, 14(3-4), 235-250.

Robert, C. R., John, M. P., & Bruce, E. P. (1987). The properties of gases and liquids. Chemical Engineering series.

Servio, P., & Englezos, P. (2002). Measurement of dissolved methane in water in equilibrium with its hydrate. Journal of Chemical & Engineering Data, 47(1), 87-90.

Sheikha, H., Pooladi-Darvish, M., & Mehrotra, A. K. (2005). Development of graphical methods for estimating the diffusivity coefficient of gases in bitumen from pressure-decay data. Energy & fuels, 19(5), 2041-2049.

Sirino, T. H., Neto, M. A. M., Bertoldi, D., Morales, R. E., & Sum, A. K. (2018). Multiphase flash calculations for gas hydrates systems. Fluid Phase Equilibria, 475, 45-63.

Sloan Jr, E. D., & Koh, C. A. (2007). Clathrate hydrates of natural gases. CRC press.

Stoessell, R. K., & Byrne, P. A. (1982). Salting-out of methane in single-salt solutions at 25 C and below 800 psia. Geochimica et Cosmochimica Acta, 46(8), 1327-1332.

Wang, Y., Han, B., Yan, H., & Liu, R. (1995). Thermal Measurements, A Selection of Papers Presented at the International and III Sino-Japanese Symposium on Thermal MeasurementsSolubility of CH4 in the mixed solvent t-butyl alcohol and water. Thermochim. Acta, 253, 327-334.

Wang, L. K., Chen, G. J., Han, G. H., Guo, X. Q., & Guo, T. M. (2003). Experimental study on the solubility of natural gas components in water with or without hydrate inhibitor. Fluid phase equilibria, 207(1-2), 143-154.

Yang, S. O., Cho, S. H., Lee, H., & Lee, C. S. (2001). Measurement and prediction of phase equilibria for water+ methane in hydrate forming conditions. Fluid Phase Equilibria, 185(1-2), 53-63.

7. RESPONSIBILITY NOTICE

The authors are the only responsible for the printed material included in this paper.